

See discussions, stats, and author profiles for this publication at: <https://www.researchgate.net/publication/51676568>

Core/Shell Cu@Ag Nanoparticle: A Versatile Platform for Colorimetric Visualization of Inorganic Anions

ARTICLE in ACS APPLIED MATERIALS & INTERFACES · SEPTEMBER 2011

Impact Factor: 6.72 · DOI: 10.1021/am200972g · Source: PubMed

CITATIONS

11

READS

40

5 AUTHORS, INCLUDING:



Jia Zhang

University of Science and Technology of China

39 PUBLICATIONS 476 CITATIONS

[SEE PROFILE](#)



Yue Yuan

University of Science and Technology of China

23 PUBLICATIONS 152 CITATIONS

[SEE PROFILE](#)

Core/Shell Cu@Ag Nanoparticle: A Versatile Platform for Colorimetric Visualization of Inorganic Anions

Jia Zhang,^{†,‡} Yue Yuan,[†] Xiaowen Xu,^{†,‡} Xiaolei Wang,[†] and Xiurong Yang^{*,†}

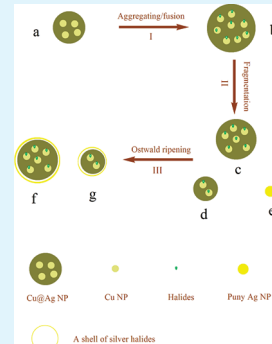
[†]State Key Laboratory of Electroanalytical Chemistry, Changchun Institute of Applied Chemistry, Chinese Academy of Sciences, Changchun 130022, Jilin, China

[‡]Graduate School of the Chinese Academy of Sciences, Beijing 100049, China

Supporting Information

ABSTRACT: Recognition and sensing of anions in aqueous media have been of considerable interest while remaining a challenging task up to date. In this document, we wish to present a simple yet sensitive method to detect inorganic anions by colorimetry based on the citrate-stabilized core/shell Cu@Ag nanoparticle (NP). It was found that the NP could discriminate some specific anions (Cl^- , Br^- , I^- , S^{2-} , and SCN^-) from a wide range of environmentally dominant anions (F^- , SO_4^{2-} , H_2PO_4^- , CO_3^{2-} , NO_3^- , etc), identified by the change in the color of the buffered NP solution or the surface plasmon resonance (SPR) absorbance band in the UV-vis spectrum. Among the recognized anions, four types of variation in the SPR absorption band were revealed. It was strongly enhanced for Cl^- and Br^- and was strongly damped for S^{2-} . For I^- , it first was slightly enhanced at lower concentrations and then gradually was damped at higher concentrations. For SCN^- , it first was slightly damped at lower concentrations and then was strongly enhanced at higher concentrations. In response to the optical change, the color of the NP solution turned from brown to bright yellow for Cl^- (1 mM), Br^- (10 μM), and SCN^- (50 μM) to brownish orange for I^- (10 μM) and to reddish orange for S^{2-} (50 μM). The reason for these phenomena was postulated by the evidence of transmission electron microscope (TEM) images, X-ray photoelectron spectroscopy (XPS), and zeta potentials. In view of the importance of anions in the environment and for human health, the Cu@Ag NP colorimetric platform may have some applications, such as discriminating household table salt (NaCl) from industrial salt (NaNO_2), testing the quality and extent of a variety of waters, and so forth.

KEYWORDS: anions, Cu@Ag nanoparticle, colorimetry, halides, sulfide, thiocyanate



INTRODUCTION

Efforts for the visual perception of anionic species in water have been animated by an appreciation that anions play a fundamental role in the ecosystem. In fact, besides DNA that carries the genetic information, the majority of enzyme substrates and cofactors involved in biological transformations are anionic in nature.¹ Like a number of metal ions, many anions exert both beneficial and detrimental effects on the environment and human health, depending upon their concentrations. A typical example is the fluoride anion that is usually added to drinking water and toothpaste to prevent the occurrence of dental carries, while chronic exposure to high levels of this anion can reversely lead to dental or even skeletal fluorosis.² An analogous effect can be attributed to another classic case of phosphate. It constitutes an essential component of the nutritional chain of the ecosystems, but it can also initiate a widespread outburst of eutrophication through rapid depletion of dissolved oxygen by aquatic microorganisms.³ In this regard, the maintenance of appropriate concentrations of anions is significant for environmentally or physiologically healthy conditions, thus emphasizing the crucial importance in the detection of these bifunctional anions, from routine analysis by trained personnel to a facile qualitative domestic test.

In view of the importance and demands, various approaches have been developed to monitor anions in water and other aqueous

media, including spectrometry or fluorometry by artificial chromophores or fluorophores,⁴ ion chromatography (IC),⁵ surface enhanced Raman scattering (SERS),⁶ electrochemical analysis,⁷ and the use of enzymatic biosensors.⁸ Inspired from supramolecular chemistry, numerous efforts have been devoted to the development of chromogenic or fluorogenic receptors for anionic species. Some of these receptors that are generally called chemosensors own the capability to recognize certain anions with remarkable selectivity; however, the majority of them can only perform in organic media, greatly limiting their applications in aqueous solutions. IC and SERS are two important modern analytical techniques that offer sensitive ways of reliable detection of anions, but the equipment is expensive and massive. Enzymatic biosensors and other electrochemical strategies feature high selectivity and low detection limit, but the main problems lie in the reproducibility. In order to deal with the drawbacks, the development of new methods that meet the requirements of simplicity, selectivity, and water-compatibility is appealing and ongoing.

Benefiting from the advance of nanotechnology, colorimetry based on precious metal nanoparticles (NPs) typified by Au and

Received: July 25, 2011

Accepted: September 26, 2011

Published: September 26, 2011

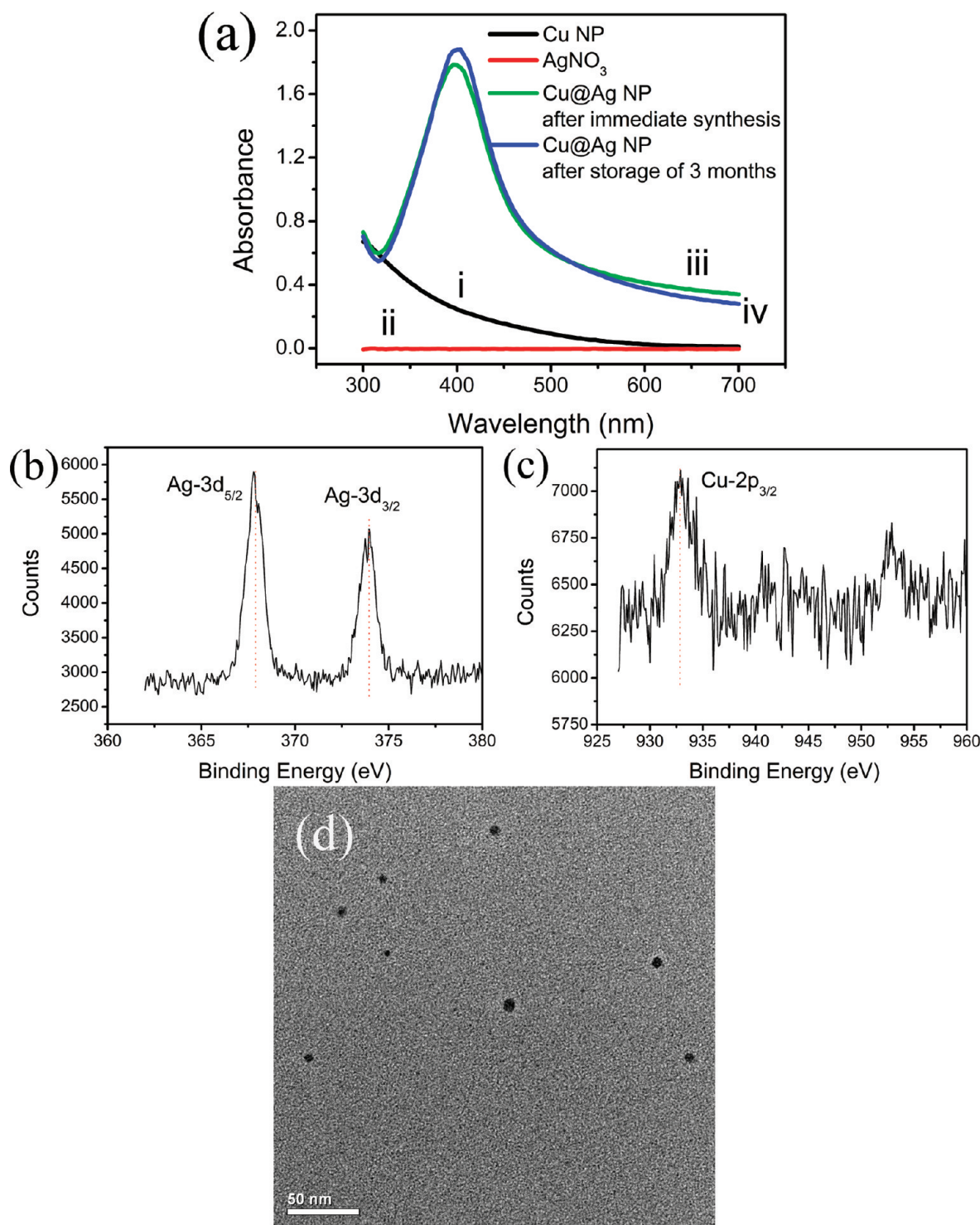


Figure 1. (a) Spectroscopic recordings of the Cu NP (i), AgNO₃ (ii), and Cu@Ag NP solutions after synthesis (iii) and storage of 3 months at room temperature (iv). XPS spectra of Ag 3d (b) and Cu 2p (c) for the Cu@Ag NP. (d) The TEM image of the morphology for the Cu@Ag NP.

Ag NPs has arisen to be one of the most important analytical methodologies for sensing a wide range of analytes, including anions.^{9–11} One of the most fascinating features of plasmonic NP-based colorimetric sensors is the simplicity of signal transduction. Generally, to make sensing realized, it is a prerequisite to chemically functionalize the plasmonic probes with appropriate receptors to ensure selectivity. Very recently, another kind of

NP-based colorimetric sensor has been developed by our group. It was found that the Cu@Au NP could recognize iodide over any other anions and cations with highly remarkable selectivity, reflected by the color of the solution changing from purple to red upon the addition of iodide.¹²

As a part of our research programs to fabricate sensors for anions as well as to extend the scope of anion recognition and

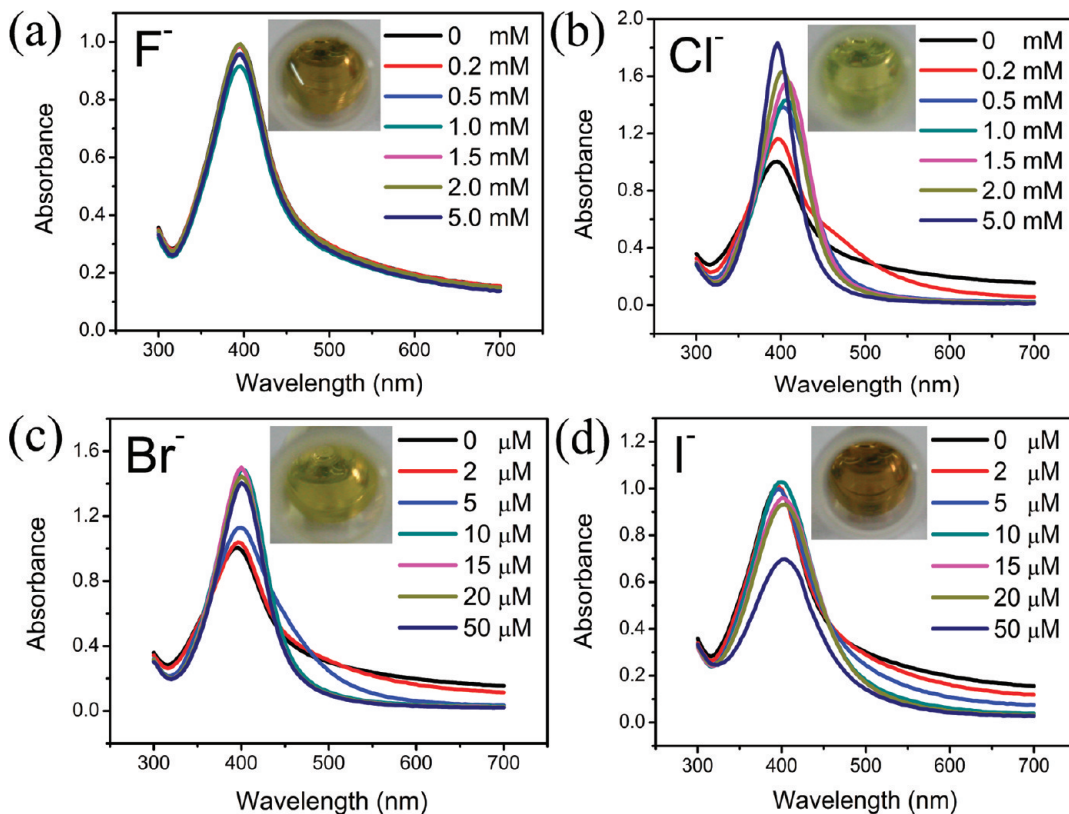


Figure 2. Concentration-dependent optical spectra for the Cu@Ag NP solution in the presence of F⁻ (a), Cl⁻ (b), Br⁻ (c), and I⁻ (d) anion for 5 min, pH 5.2. The insets are the photographs showing respective colorimetric responses.

sensing by plasmonic nanoparticles, here, we demonstrate a new colorimetric platform for anions using the citrate-stabilized core/shell Cu@Ag NP. Replacing HAuCl₄ for the Cu@Au NP with AgNO₃, we synthesized like-charged Cu@Ag NP. In comparison with the impressive selectivity of Cu@Au NP for iodide, it was found that the new Cu@Ag NP had totally different ability toward the recognition of anions. Detailed information is to be presented in the following section.

■ EXPERIMENTAL SECTION

Reagents. CuSO₄·5H₂O and NaBH₄ were purchased from Sigma-Aldrich (USA). AgNO₃ was purchased from Acros Organics (USA). Analytical grade sodium citrate and other inorganic chemicals were obtained from Beijing Chemical Reagent Co. (China). They were all used without additional purification. Phosphate buffer solutions (PBS) with varied pH values were prepared by varying the ratio of 10 mM Na₂HPO₄ to 10 mM KH₂PO₄. Milli-Q water (18.2 MΩcm) was used throughout the experiment. Unless specified, the experiment was conducted at 14 ± 2 °C.

Apparatus. UV-vis absorption spectra were recorded with a Cary 50 UV-vis spectrometer (Varian). Photographs were taken with a CanonPSA490 digital camera (Canon). Transmission electron microscope (TEM) images were acquired using a Tecnai G2 F20 (FEI) transmission electron microscope operated at 200 kV. TEM samples were prepared by applying drops of the NP solutions to carbon-coated copper grids in contact with filter paper. Such a process was made to prevent coagulation of particles. The X-ray photoelectron spectroscopy (XPS) samples on highly cleaned silicon wafers were analyzed by an ESCALAB MK II spectrometer (VG Scientific) with Al K α radiation as the X-ray source. Peak positions were internally referenced to the C1s

peak at 284.6 eV. Zeta potential of the NP solutions was examined by a Malvern Zetasizer nano instrument (Malvern).

Synthesis Procedure. As an analogy to the synthesis of Cu@Au NP, in a typical experiment, 40 mL of water was mixed with aqueous solutions of CuSO₄ (100 μ L, 0.1 M) and sodium citrate (100 μ L, 0.1 M). Afterward, 1 mL of freshly prepared NaBH₄ (7.6 mg in 4 mL of H₂O) was injected into the stirring system rapidly. About 15 min later, aqueous AgNO₃ solution (100 μ L, 0.1 M) was added, and the solution was kept stirring for 20 min. The final solution was stocked at ambient environment for a minimum of 24 h before its further application.

■ RESULTS AND DISCUSSIONS

Synthesis and Characterization of the Cu@Ag NP. Figure 1a shows the UV-vis spectra recording of the synthesis procedure. Likewise, the Cu NP solution exhibited no absorption peak near 560 nm (Figure 1a,i) where the characteristic surface plasmon resonance (SPR) absorption of Cu NP usually appears, suggesting an infinitesimal size below 2 nm.¹³ Upon the addition of AgNO₃, the color of the solution changed from pale yellow to brown. Concomitantly, a strong absorption peak occurred at 396 nm (Figure 1a,iii), which was related to the well-known SPR absorption of Ag NP. To be cautious, we cannot infer from the optical spectra that silver ion was transformed completely to Ag NP since it had no absorbance in the spectrum range (Figure 1a,ii). However, there are still two points we can make clear on the basis of an understanding of the synthesis of Cu@Au NP. One is the transformation of Ag⁺ ion by a synergy of NaBH₄ reduction and the galvanic displacement reaction between Ag⁺ ion and Cu NP; the other is the deposition of Ag clusters onto Cu NP to obtain core/shell Cu@Ag NP. The stability of the nanoparticle was

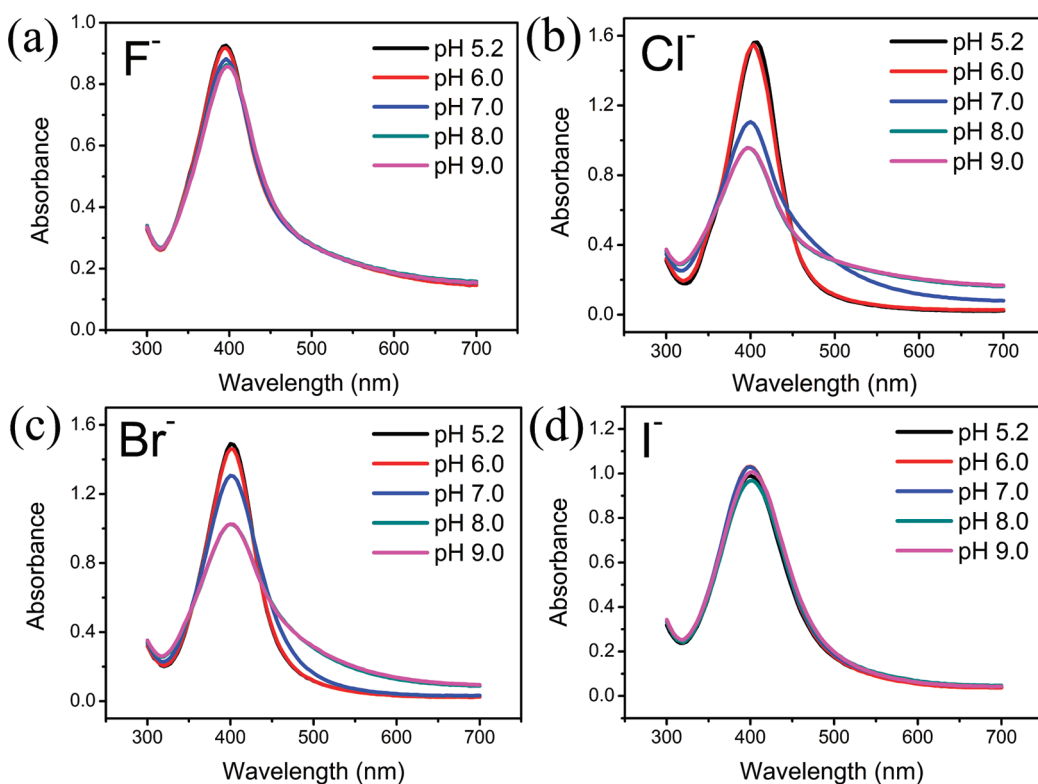


Figure 3. pH-dependent optical spectra for the Cu@Ag NP solution in the presence of (a) F^- (1 mM), (b) Cl^- (1 mM), (c) Br^- (10 μM), and (d) I^- (10 μM) anion for 5 min.

evaluated by recording the spectrum after 3 months of storage (Figure 1a,iv). Little change was observed, indicating that it owns a much better capacity against sedimentation compared to the like-charged Cu@Au NP.

X-ray photoelectron spectroscopy (XPS) was further used to analyze the exact elemental valence of the nanoparticle. The spectrum for Ag revealed a typical Ag 3d doublet with the binding energy (E_B) of Ag 3d_{5/2} located at 367.9 eV and a doublet splitting of 6 eV (Figure 1b), in accordance with the zero valence of Ag atom.¹⁴ Meanwhile, the Cu spectrum showed a E_B at 932.8 eV associated with Cu 2p_{3/2} (Figure 1c), which marked metallic Cu (Cu⁰) or Cu₂O.¹⁵ Under the reductive environment of NaBH₄, it is reasonable to believe that the metallic Cu (Cu⁰) was responsible for the binding energy. Additionally, the broad satellite peaks around 940–945 eV appeared due to the generation of Cu²⁺ ion during the galvanic displacement reaction. This is analogous to that in the case of Cu@Au NP.

To get insight into the morphology of the nanoparticle, transmission electron microscopy (TEM) was studied, as shown in Figure 1d. In vivid comparison with the interconnected, irregular geometry of the Cu@Au NP, the Cu@Ag NP appeared in a well-defined sphere as a highly separate state, with size falling dominantly within the range of 4–9 nm. This is interesting to realize, and it explains the differed capacity of both NPs against sedimentation (the Cu@Ag NP was stable as of synthesis but the Cu@Au NP was observed with precipitate after 1 month of storage). Such difference in morphology may be explained by the clear difference in the oxidative potentials of AuCl_4^- and Ag⁺ ions. Having a less oxidative potential,¹⁶ Ag⁺ ion would be less reactive for both the reductions (vide supra), implying a slower encapsulation of Cu NP by Ag⁺ ion to form single, discrete Cu@Ag NP.

From the above results, we cannot conclude the core/shell structure of the nanoparticle that we obtain. X-ray diffraction (XRD) data of the nanoparticle failed to be collected because it could not be separated by centrifugation under the current experimental conditions. However, on the basis of a comparison of synthesis between Cu@Au NP and the present NP, it is reasonable to suppose the core/shell structure of the nanoparticle.

UV-vis Spectroscopic Investigation of Halides Recognition. Previous studies revealed that the SPR absorption bands of Ag nanostructures were sensitive to the presence of adsorbed substances, especially anions.^{17–20} In this work, we commenced to investigate the sensitivity of the Cu@Ag NP toward halides. Figure 2 shows the concentration-dependent optical spectra of the buffered NP solution (pH 5.2) for the four halides. The results according to the SPR peak absorption can be classified as three types of variation, with no change for F^- , strongly enhanced for Cl^- and Br^- , and first slightly enhanced and then gradually damped for I^- . Moreover, Br^- manifested a much higher sensitivity than Cl^- , although it had a less maximum absorbance than Cl^- . Insofar as we know, it is the first discovery of enhancement in SPR absorbance for plasmonic nanoparticles by halides. The spectroscopic responses were supplemented by the observation of the visible color changes of solutions. It was originally brown for F^- (1 mM), bright yellow for Cl^- (1 mM) and Br^- (10 μM), and brownish orange for I^- (10 μM) (Insets of Figure 2), respectively. Control experiments were conducted using citrate-stabilized Ni@Ag NP and Ag colloid. No analogous changes were observed in the SPR absorption band (Figure S1, Supporting Information) or color of the solution for neither of them, suggesting coordination of the Cu NP core and Ag atoms shell for the recognition of the halides. Therefore, the Cu@Ag NP can

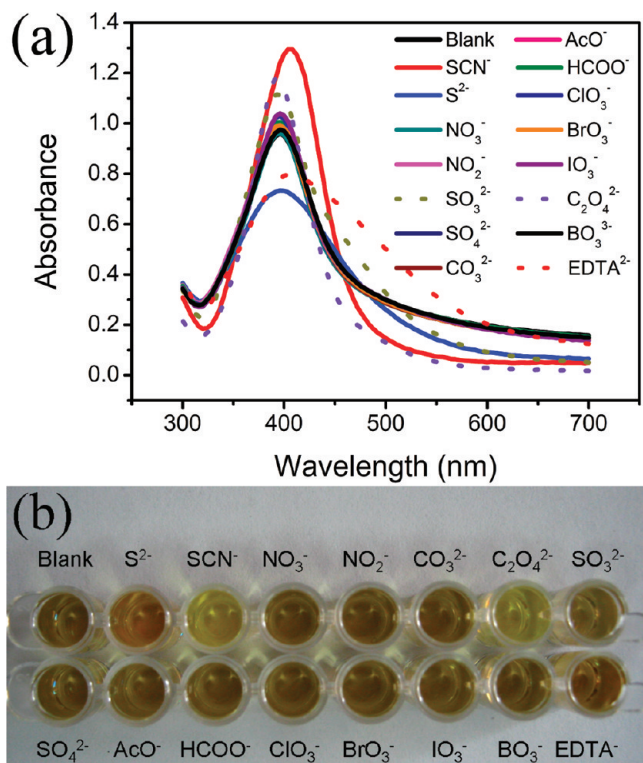


Figure 4. (a) Spectroscopic recordings of the Cu@Ag NP solution after interaction with anions and (b) the photograph showing the colorimetric response, pH 5.2.

be regarded as a new colorimetric platform for the sensitive detection of halides.

The pH-dependent response of the platform on the addition of the halides was studied, as shown in Figure 3. Likewise, three types of change were revealed. For F⁻ (1 mM), no apparent change in the SPR band was observed, except a little attenuation of the absorption peak with increasing pH (Figure 3a). For Cl⁻ (1 mM) and Br⁻ (10 μ M), the enhancement in SPR absorption behaved the same at pH 5.2 and 6.0, weakened dramatically for Cl⁻ and less dramatically for Br⁻ at pH 7.0, and was nearly absent above pH 8.0 for both anions (Figure 3b,c). For I⁻ (10 μ M), the solution pH exerted little effect on the optical response (Figure 3d). From the results, it seems that the influence of pH on the sensing sensitivity of the platform for the halides is determined by the strength of Ag–halide bond, with the less/most appreciable extent for I⁻/Cl⁻ relative to the highest/lowest strength of Ag–I/Ag–Cl bond. Besides the pH dependence, we also found that the recognition event was kinetically fast, manifested by the time-dependent spectra (Figure S2, Supporting Information). To ensure reproducibility, 5 min was set for the sensing of halides in the experiment.

To better understand the interaction between the Cu@Ag NP and halides, a series of experiments were carried out. First, several groups of mixtures of halide anions were added to the NP solution (Figure S3a, Supporting Information). Compared with the spectra for the sole addition of one kind, it can be seen that mixture of Cl⁻ and Br⁻ elicited a response between those for individual ones, and meanwhile, mixtures of (i) Cl⁻ and I⁻, (ii) Br⁻ and I⁻, and (iii) Cl⁻, Br⁻, and I⁻ elicited responses similar to that for single I⁻. Second, Br⁻ or I⁻ was initially added for 5 min and followed by the addition of Cl⁻ or Br⁻ (Figure S3b, Supporting Information).

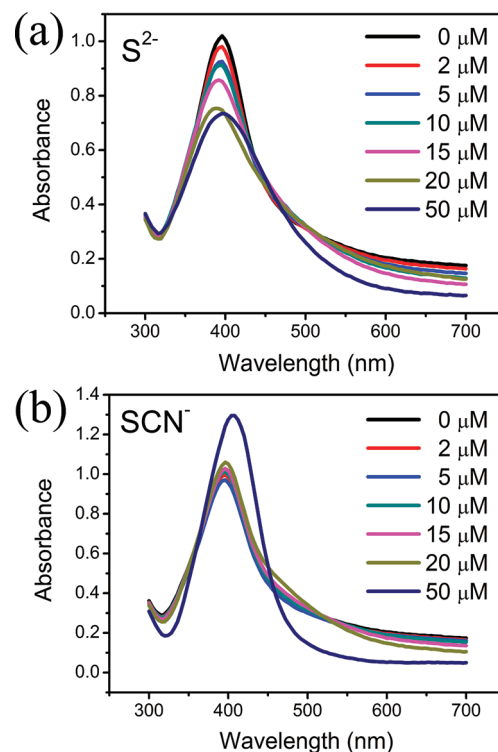


Figure 5. Concentration-dependent optical spectra for the Cu@Ag NP solution in the presence of S²⁻ (a) and SCN⁻ (b) anion for 5 min, pH 5.2.

It was found that the successive addition of Cl⁻ after Br⁻ elicited a response similar to that for single Cl⁻ and, meanwhile, the successive addition of Cl⁻ or Br⁻ after I⁻ did not make a difference from that for single I⁻. Third, Cl⁻ or Br⁻ was initially added for 5 min and followed by the addition of Br⁻ or I⁻ (Figure S3c, Supporting Information). It was found that the successive addition of Br⁻ after Cl⁻ elicited SPR absorbance somewhat larger than that for single Cl⁻, and meanwhile, the successive addition of I⁻ after Cl⁻ or Br⁻ elicited similar response, either of which laid between those for single I⁻ and Cl⁻ or Br⁻. From the results, it is clear that I⁻ can greatly interfere with the enhancement effect of Cl⁻ and Br⁻, irrespective of how it is added. For Cl⁻ and Br⁻, no obvious synergy of SPR band was observed, either in the mixture or by sequential addition. The possible reason may be that the interaction between the NP and individual Cl⁻ or Br⁻ almost finished at the present concentrations (Figure 3b,c), precluding the observation of potential synergy of enhancement in SPR.

UV-vis Spectroscopic Investigation of Other Anions Recognition. We carried on the experiment by testing the sensitivity of the platform toward the recognition of other anions. Figure 4a shows the spectra of the buffered NP solutions in the presence of a wide range of other anions. Correspondingly, it revealed four types of variation by the SPR absorption, with degree-differed enhancement effect as Cl⁻ and Br⁻ for SCN⁻ (50 μ M), SO₃²⁻ (1 mM), and C₂O₄²⁻ (1 mM), damping effect as I⁻ for S²⁻ (50 μ M), a different damping effect for EDTA²⁻ (1 mM), and insignificant effect for the other anions (all 1 mM). Figure 4b shows the colorimetric responses of the NP solutions. The color of the solution changed from brown to yellow for SCN⁻ and C₂O₄²⁻, to brownish orange for SO₃²⁻, and to reddish orange for S²⁻ and EDTA²⁻, and there was no noticeable change for the other anions. For Ag nanoprisms, the SPR absorption peak shifted in the

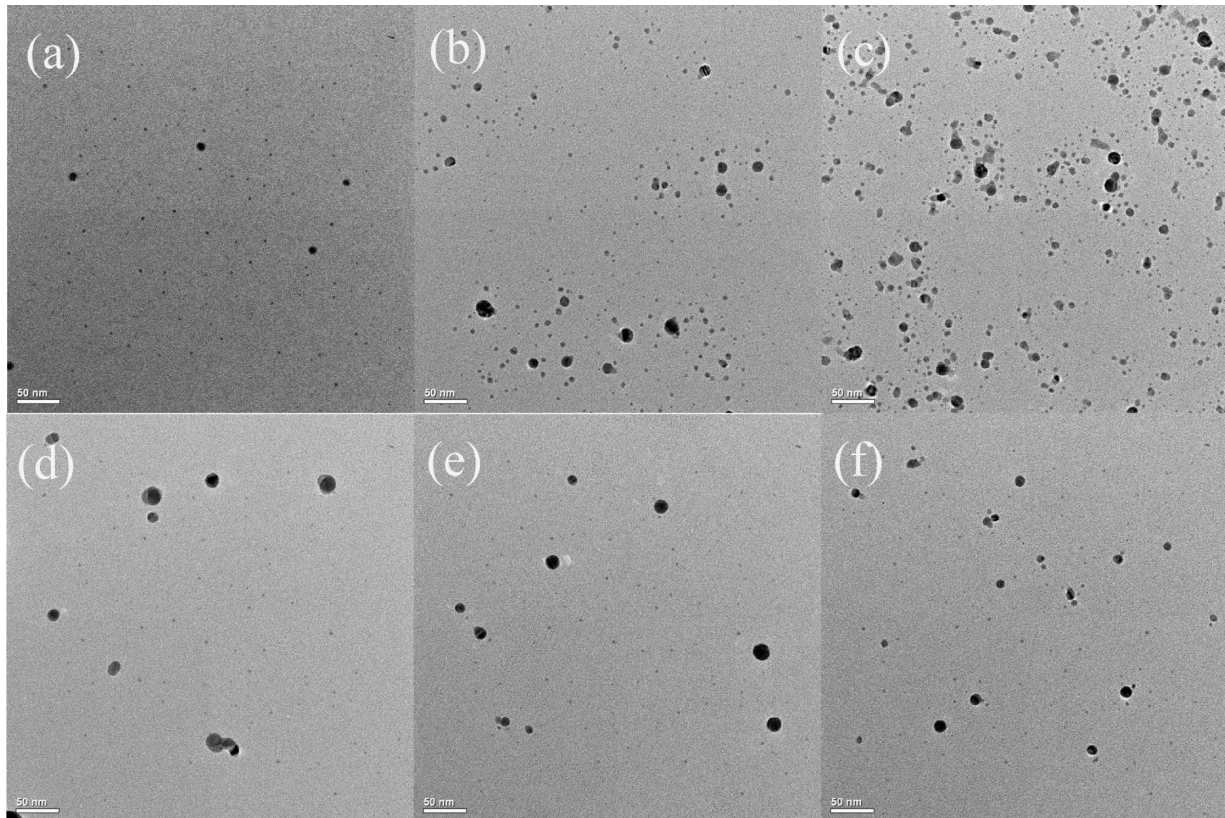


Figure 6. Typical TEM images of the Cu@Ag NP after interaction with Cl⁻ (a and d), Br⁻ (b and e), and I⁻ (c and f) for 5 min (a–c) and 2 h (d–f). The scale bar represents 50 nm.

presence of phosphate anion.¹⁷ In the present study, the phosphate buffer was used, since we found that the Cu@Ag NP did not respond to phosphate (Figure S4, Supporting Information). Owing to the higher sensitivity that S²⁻ and SCN⁻ manifested, we focused on the two anions and investigated their concentration-dependent spectral changes. Figure 5a shows the optical changes of the NP in the presence of S²⁻. Along with the increase of concentration, the SPR peak absorption decreased gradually, in synchrony with the decrease of absorbance at higher wavelength. Meanwhile, the peak position made a dynamic blue-shift until 20 μ M and shifted inversely at 50 μ M. Such change in SPR absorption upon the addition of sulfide was also observed for silver colloid.²³ Figure 5b shows the optical changes of NP in the presence of SCN⁻. Unlike the damping for S²⁻, the SPR peak absorption attenuated slightly at the initially small concentration (until 5 μ M) and then enhanced slightly until 20 μ M and remarkably at 50 μ M. Mixtures of S²⁻ or SCN⁻ with halides were also studied for the interaction with the nanoparticle (Figure S5, Supporting Information). It uncovered that S²⁻ can interfere with the enhancement effect of Cl⁻ and Br⁻ alike I⁻ but with a less extent and, meanwhile, it can cooperate with I⁻ to produce a synergy of damping. For SCN⁻, it showed that it could not compete with halides to interact with the nanoparticle, since the spectra for mixtures containing it and halides were almost the same with those for respective halides.

Mechanism for the Recognition of Anions by the Cu@Ag NP. To elucidate the recognition mechanism, more analysis was performed, exemplified by the recognition of halides. Although the interaction between the NP and halides appeared to reach the end point within 5 min, we found that the spectra did not remain

stable (Figure S6, Supporting Information). (Note: In this test, 2.0 mL clear microtube (homopolymer, boil-proof) from Axygen Scientific Co. was used. It could perfectly prevent the adsorption of nanoparticles onto the sidewall of tube, guaranteeing the accuracy of the results.) Along with time, there was a gradual redshift in the SPR absorption peak position and decrease of absorbance. More immediate changes can also be observed by increasing the concentration of anions (Figure S7, Supporting Information). For I⁻, a steep absorption threshold at 425 nm, indicative of AgI, appeared first at a concentration of 100 μ M. It is analogous to that for the plasmon damping of Ag colloid by the adsorption of I⁻.¹⁸ By a combination of the fast kinetic optical change within 5 min and the considerably decelerated change after recognition, we can infer that two distinctive processes are to be accounted for. Corresponding to the optical spectra, the morphology of the nanoparticle after interaction for 5 min and 2 h was characterized by transmission electron microscope (TEM), as shown in Figure 6. Compared with the native one (Figure 1d), the NP after recognition for 5 min barely changed the shape and generally had a larger size, with diameters being within 9–10 nm for Cl⁻, 5–18 nm for Br⁻, and 5–15 nm for I⁻ (Figure 6a–c). In addition, it is noteworthy that a large number of puny particles with 2–3 nm average diameter appeared in the images. After 2 h of interaction, the size of the larger NP became larger continually, being dominantly within 12–20 nm for Cl⁻, 8–18 nm for Br⁻, and 8–15 nm for I⁻ (Figure 6d–f). Meanwhile, the puny particles still existed, while minimizing in number appreciably. It is reasonable to attribute the enlargement of NP in size to the synchronous decrease of the puny particles in number. Therefore, the baffling question is how did the puny particles

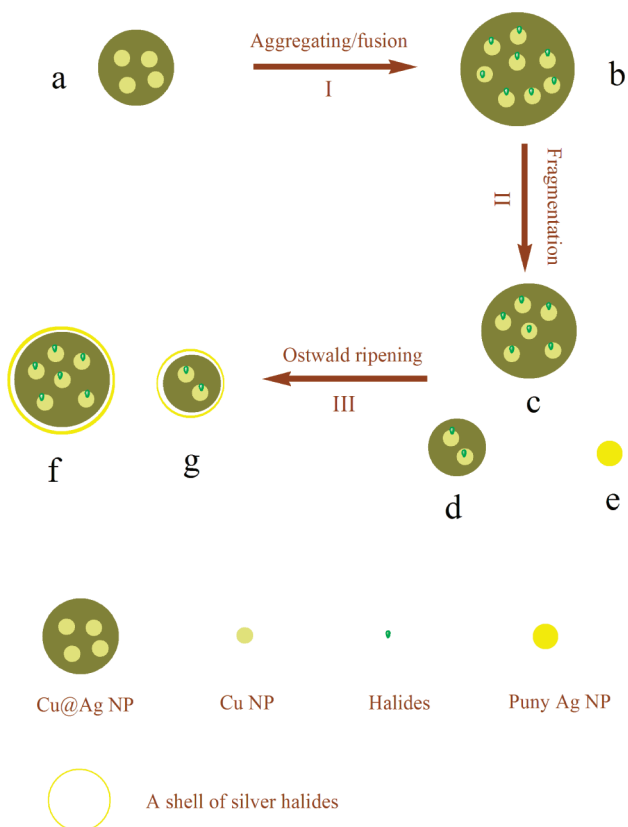


Figure 7. Schematic representation of the mechanism for the recognition of anions by the Cu@Ag NP. Note: To discriminate the shell of silver halides from the transformed NPs (f and g), a different color is used and a small space is inserted between them.

develop, what did they represent, and how could we correlate the optical spectra with the TEM observations. In the previous study, a mechanism of aggregating/fusion, fragmentation, and reorganization of atoms was proposed,¹² and here, we present a somewhat different mechanism for the anions recognition by the Cu@Ag NP that is represented in Figure 7, on the basis of the optical spectra and TEM results. The transformation can be divided to three steps, much alike the previous. The adsorption of halide onto the surface of NP (Figure 7a) occurs rapidly due to the high affinity of Ag–halide bond or, to put it in another way, the low solubility of silver halide compound. The citrate ion is displaced due to the halide adsorption, causing a tremendous decrease of the zeta potential, which initiates the aggregating/fusion of NP (Figure 7, I). It is anticipated that, during the aggregating/fusion process, the inclusion and adsorption of halide on the surface of Cu NP core will happen. Owing to the inclusion, the zeta potential of the fusing intermediate (Figure 7b) reversely increases and it leads to a *prompt* fragmentation (Figure 7, II), hence generating smaller Cu@Ag NPs (Figure 7c,d) and the puny Ag NP (Figure 7e). With progression of the interaction, the number of Ag NP minimizes by the Ostwald ripening process (Figure 7, III), synchronized by the formation of a homogeneous shell of more than one monolayer of silver halide on the surface of the new particles (Figure 7c,d) to produce bigger particles (Figure 7f,g). The mechanism should also be applied to the recognition of other anions, such as sulfite, thiocyanate, and oxalate.

To induce the aggregating/fusion process, it is a prerequisite that the displacement of citrate by anions reduces the zeta

potential of NP. This occurs when the anions adsorb to silver stronger than citrate, which is acknowledged to be determined by the relative strength of Ag–anion bond, i.e., the solubility of silver salts of these anions.⁶ The recognition of the anions such as sulfate, nitrate, and acetate was negative, suggesting that they failed to displace citrate, which can be verified by the fact that their respective silver salts have higher solubility than silver citrate. Conversely, the NP platform can recognize the anions such as halides (F[−] except), sulfide, sulfite, thiocyanate, and oxalate in that their respective silver salts have lower solubility than silver citrate.^{6,21} The synthesis of Cu NP by NaBH₄ reduction in the presence of the three halides was performed to obtain clear solutions while, without them, black precipitation was obtained. It clearly manifested the adsorption of the halides on the surface of Cu NP, and it should be applied to the other anions recognized. Zeta potential data also provided the evidence of the adsorption of halides. It was found that the zeta potential of NP solutions increased from −31.8 eV to −38.3, −43.3, and −38.9 eV after interaction with Cl[−], Br[−], and I[−], respectively. According to the spectra recordings (Figure S2, Supporting Information), the process II is remarkably fast, since the spectra changed dramatically within 1 min and was stable within 5 min. We believe that the puny Ag NP derived from the process II is responsible for the enhancement in SPR for Cl[−] and Br[−]; however, it does not cause similar effect for I[−] because I[−] damps the SPR absorbance of the puny Ag NP strongly and quickly.¹⁸ The most profound damping of SPR band of Ag colloid by I[−] was also observed in our experiment (Figure S1b, Supporting Information). We thus attribute the extent of damping effect by anions to the relative strength of Ag–anion bond, with the strongest damping (i.e., I[−]) corresponding to the highest strength and the weakest damping (i.e., Cl[−]) corresponding to the lowest strength. Appreciating this relationship, one can understand the spectral observation that, after recognition for 5 min, the maximum SPR absorption occurred for Cl[−] and the minimum occurred for I[−] (Figure 2b–d). Besides, the solubility decides inversely the extent (or sensitivity) of the recognition. For the anions showing enhancement effect, there is a hierarchy for the sensitivity of anions with the same charge number that follows the order of Br[−] > SCN[−] > Cl[−], in good agreement with a gradual increase in solubility of the respective silver salts.²¹ In the other hand, the charge number of anion also inversely influences the extent of recognition. It has been found that C₂O₄^{2−} and SO₃^{2−} can be recognized with a lower sensitivity than Cl[−], and PO₄^{3−} cannot even be recognized, although their respective silver salts are more insoluble than AgCl, according to the solubility product constant.²¹ Such paradox may be in the fact that the ion product of silver anion salt (i.e., [Ag⁺]ⁿ × [(Anion)^{n−}]) decreases drastically with the increase of charge number of anion (the *n*). We think that only if the *ion product* of silver anion salt is above its corresponding *solubility product* can the displacement of citrate occur, and meanwhile, the discrepancy of the two products dictates the degree of the citrate displacement, which in turn determines the sensitivity of recognition. In this regard, the sensor offers a perfect platform to study the relative strength of silver–anion bond. For the recognition of iodide by the Cu@Au NP, the process of reorganization of atoms almost finished within 20 min,¹² but this Ostwald ripening process is kinetically much decelerated, as evidenced by the spectral results. A homogeneous shell of silver halides rather than sporadic attached particles formed around the transformed NPs after fragmentation, identified by the TEM and X-ray photoelectron microscope (XPS)

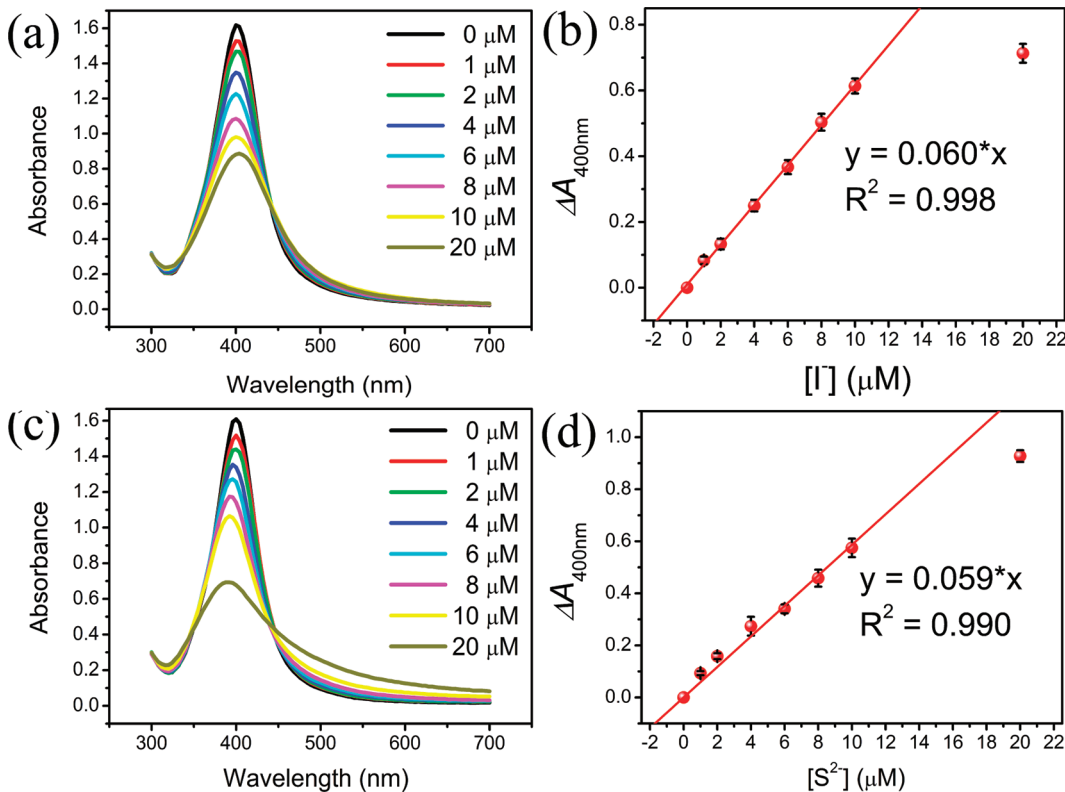


Figure 8. (a) Optical spectra for the Cu@Ag NP solution after interaction with mixtures of various concentrations of iodide and chloride (1 mM) for 5 min, pH 5.2. (b) The correlation of the relative absorbance at 400 nm with the concentration of iodide. (c) The optical spectra for the Cu@Ag NP solution after interaction with mixtures of various concentrations of sulfide and chloride (1 mM) for 5 min, pH 5.2. (d) The correlation of the relative absorbance at 400 nm with the concentration of sulfide.

analysis. No sign of particles attached on the surface of the new NP was observed (Figure S8, Supporting Information), suggesting a homogeneous mantled shell around it. Besides, attached silver halide particles could hardly disturb the silver SPR band.¹⁸ The change in the chemical environment of the elements was further supported by XPS. Compared with the binding energy for the native NP, there were shifts toward lower energies for both the characteristic silver peak (Ag-3d_{5/2}) and halides (Cl-2p_{3/2}, Br-3d_{5/2}, and I-3d_{5/2}) after recognition (Figure S9a,c–e, Supporting Information), implying the detection of silver halides.²² Moreover, strong peaks located at around 377 eV emerged, which corresponded with the surface plasmon loss peak of silver.²³ All these results definitively verified the formation of silver halides on the surfaces of the transformed NPs. Here, we lack the X-ray diffraction (XRD) data to trace the possible morphological change of Cu NP after interaction, since neither the native NP nor the transformed ones could be separated by centrifugation, even increasing the ionic strength of the solution with the addition of salt (e.g., Na₂SO₄). So, on the basis of the previous mechanism,¹² it is better, supposing that the Cu NP remains stable in geometry. Please note that the new NPs represented as Figure 7f,g are confined to the transformation within 2 h, since the geometry of particles after this period of time was not analyzed and it might change to another kind of shape.^{24,25} It is well acknowledged that the oxidation of silver atoms in the presence of halides is coupled to proton reduction,²⁶ suggesting a connection of the recognition with the solution pH, in consistence with the optical spectra (Figure 3). Besides the variations in binding energy for silver and halides, the spectra

relative to copper after interaction were also recorded. Little shift occurred to the characteristic copper peak (Cu-3p_{3/2}), indicating no change in the valence of Cu for the transformed NPs. However, there was considerable decrease of Cu to Ag atomic ratio (Cu/Ag) for the new NPs compared with the native NP, suggesting either a decrease in Cu amount or an increase in Ag amount. Under this circumstance, an increase in Ag amount is more justified, matching well with the formation of a shell of silver halides.

Detection of Certain Anions. Until now, the Cu@Ag NP has been identified as a new platform for the selective detection of some anions over a wide range of environmentally dominant anions, such as fluoride, sulfate, and phosphate. The detection of chloride succumbs to the interference problems from heavier halides (Br⁻ and I⁻) and sulfide due to their superior affinity to silver. However, such limitations can be of little importance under certain circumstances when the concentrations of these anions are very low, for example, in the commercial sports drink²⁷ or the tap water. Besides, this sensor manifests a remarkably high selectivity of chloride over phosphate, where it is superior to the Ag nanoprisms¹⁷ that cannot discriminate the two anions. Free from any interference, the limit of detection for chloride by the NP sensor is 0.1 mM with a UV-vis spectrometer and appreciable color change of solution can be observed at 0.2 mM with the naked eye. Thus, the Cu@Ag NP platform appears to allow for the direct assay of chloride anion in water or other aqueous solutions. Here, two tap water samples subjected with no pretreatment were analyzed by the sensor for the detection of chloride. No chloride was detected unfortunately

due to the limitation of the detection limit for chloride by the sensor. However, the percent recoveries were satisfactorily over 90%, which implied the usefulness of the sensor for the qualitative or semiquantitative chloride assay in a simple and straightforward way under certain circumstances.

Besides the chloride sensing, iodide and sulfide were detected alternatively in the presence of chloride by taking advantage of the fact that the enhancement in SPR by chloride is severely interfered by iodide or sulfide. Mixtures containing various concentrations of iodide or sulfide and chloride (1 mM) were added to the NP solution for 5 min, and the optical spectra were recorded, as shown in Figure 8a,c. The SPR absorbance decreased gradually with increasing concentration of the anion target, showing a new interesting way of correlation between them in contrast with that in the absence of chloride (Figures 2d and 5a). By correlating the relative absorbance at 400 nm with the concentration, two analogous linear lines with similar slope were obtained, as shown in Figure 8b,d. The new way of detection has a better sensitivity, with limits of detection being 0.25 μM for both anions. Interference tests revealed that either of the two anions would be the dominant interference for the detection of the other (Figure S10, Supporting Information). It is expected since both anions can damp the plasmon absorption in an analogous way.

CONCLUSIONS

In summary, we have demonstrated a new platform for colorimetric recognition of anions based on the core/shell Cu@Ag NP. It can discriminate some anions such as halides (except fluoride), sulfide, and thiocyanate from a wide spectrum of environmentally relevant anions with high sensitivity. Two main types of variation in plasmon absorption were discovered, with enhancement effect for Cl^- , Br^- , and SCN^- and damping effect for I^- and S^{2-} . To the best of our knowledge, it is the first time to observe the enhancement in SPR of plasmonic nanoparticles induced by anions. Besides, this nanoparticle serves as a perfect platform to study the relative strength of anion–silver bond. A mechanism was proposed, on the basis of the results associated with optical spectra, TEM, XPS, and zeta potential. Given the great effects of anions exerting on the environment, human health, and industrial processes, this platform may have some applications, like water quality control, discrimination of edible table salt from industrial salt, and direct analysis of chloride anion in commercial sports drinks and tap water.

ASSOCIATED CONTENT

Supporting Information. Additional figures as noted in the text. This material is available free of charge via the Internet at <http://pubs.acs.org>.

AUTHOR INFORMATION

Corresponding Author

*E-mail: xryang@ciac.jl.cn. Fax: +86 431 85269278.

ACKNOWLEDGMENT

This work was supported by the National Natural Science Foundation of China (No. 20890020) and the National Key Basic Research Development Project of China (Nos. 2010CB933602 and 2007CB714500).

REFERENCES

- (1) Beer, P. D.; Gale, P. A. *Angew. Chem., Int. Ed.* **2001**, *40*, 486–516.
- (2) Wade, C. R.; Broomsgrove, A. E. J.; Aldridge, S.; Gabbaï, F. P. *Chem. Rev.* **2010**, *110*, 3958–3984.
- (3) Sessler, J. L.; Cho, D.; Lynch, V. *J. Am. Chem. Soc.* **2006**, *128*, 16518–16519.
- (4) Martínez-Máñez, R.; Sancenón, F. *Chem. Rev.* **2003**, *103*, 4419–4476.
- (5) Demkowska, I.; Polkowska, Z.; Namiesnik, J. *J. Chromatogr., B* **2008**, *875*, 419–426.
- (6) Bell, S. E. J.; Sirimuthu, N. M. S. *J. Chromatogr., A* **2005**, *109*, 7405–7410.
- (7) Isaac, A.; Livingstone, C.; Wain, A. J.; Compton, R. G.; Davis, J. *Trends Anal. Chem.* **2006**, *25*, 589–598.
- (8) Yablotskii, K. V.; Shekhovtsova, T. N. *J. Anal. Chem.* **2010**, *65*, 660–673.
- (9) Durocher, S.; Rezaee, A.; Hamm, C.; Rangan, C.; Mittler, S.; Mutus, B. *J. Am. Chem. Soc.* **2009**, *131*, 2475–2477.
- (10) Daniel, W. L.; Han, M. S.; Lee, J.; Mirkin, C. A. *J. Am. Chem. Soc.* **2009**, *131*, 6362–6363.
- (11) Xiao, N.; Yu, C. X. *Anal. Chem.* **2010**, *82*, 3659–3663.
- (12) Zhang, J.; Xu, X.; Yang, C.; Yang, F.; Yang, X. *Anal. Chem.* **2011**, *83*, 3911–3917.
- (13) Brege, J. J.; Hamilton, C. E.; Crouse, C. A.; Barron, A. R. *Nano Lett.* **2009**, *9*, 2239–2242.
- (14) Thomas, S.; Nair, S. K.; Jamal, E. M. A.; Al-Harthi, S. H.; Varma, M. R.; Anantharaman, M. R. *Nanotechnology* **2008**, *19*, 075710.
- (15) Sarkar, A.; Manthiram, A. *J. Phys. Chem. C* **2010**, *114*, 4725–4732.
- (16) Lide, D. R. *Handbook of Chemistry and Physics*, 89th ed.; CRC Press: Boca Raton, FL, 2008, p 8–20.
- (17) Jiang, X.; Yu, A. *Langmuir* **2008**, *24*, 4300–4309.
- (18) Linnert, T.; Mulvaney, P.; Henglein, A. *J. Phys. Chem.* **1993**, *97*, 679–682.
- (19) An, J.; Tang, B.; Zheng, X.; Zhou, J.; Dong, F.; Xu, S.; Wang, Y.; Zhao, B.; Xu, W. *J. Phys. Chem. C* **2008**, *112*, 15176–15182.
- (20) Hsu, M.; Cao, Y.; Wang, H.; Pan, Y.; Lee, B.; Huang, C. *ChemPhysChem* **2010**, *11*, 1742–1748.
- (21) Lide, D. R. *Handbook of Chemistry and Physics*, 89th ed.; CRC Press: Boca Raton, FL, 2008, p 8–119.
- (22) Grzelczak, M.; Sánchez-Iglesias, A.; Rodríguez-González, B.; Alvarez-Puebla, R.; Pérez-Juste, J.; Liz-Marzán, L. M. *Adv. Funct. Mater.* **2008**, *18*, 3780–3786.
- (23) Tachibana, Y.; Kusunoki, K.; Watanabe, T.; Hashimoto, K.; Ohsaki, H. *Thin Solid Films* **2003**, *442*, 212–216.
- (24) Cheng, W.; Dong, S.; Wang, E. *Angew. Chem., Int. Ed.* **2003**, *42*, 449–452.
- (25) Wang, J.; Li, Y.; Huang, C. *J. Phys. Chem. C* **2008**, *112*, 11691–11695.
- (26) Mulvaney, P. *Langmuir* **1996**, *12*, 788–800.
- (27) Yoo, D.; Gross, D. E.; Lynch, V. M.; Lee, C.; Bennett, P. C.; Sessler, J. L. *Chem. Commun.* **2009**, 1109–1111.